

Basic Divertor Operation in ITER-FEAT

A. S. Kukushkin 1), G. Janeschitz 1), A. Loarte 2), H. D. Pacher 3), D. Coster 4),
G. Matthews 5), D. Reiter 6), R. Schneider 7), V. Zhogolev 8)

- 1) ITER JCT, Boltzmannstr. 2, 85748 Garching, Germany
- 2) EFDA, Close Support Unit, Garching, Germany
- 3) INRS-Energie et Matériaux, Varennes, Québec, Canada
- 4) Max-Planck-Institut für Plasmaphysik, Garching, Germany
- 5) JET Joint Undertaking, Abingdon, United Kingdom
- 6) FZ Jülich, Jülich, Germany
- 7) Max-Planck-Institut für Plasmaphysik, Greifswald, Germany
- 8) RSC “Kurchatov Institute”, Moscow, Russia

e-mail contact of main author: kukusha@itereu.de

Abstract. This paper summarises the modelling studies of steady-state divertor operation being performed for the ITER-FEAT design. Optimisation of the divertor geometry reveals the importance of the proper target shape for a reduction of the peak power loads. A high gas conductance between the divertor legs is also essential for maintaining acceptable conditions in the outer divertor which receives higher power loading than the inner. Impurity seeding, which would be necessary if tritium co-deposition concerns preclude the use of carbon as plasma-facing material, can ensure the required high radiation level at acceptable Z_{eff} , and the divertor performance is not very sensitive to the choice of the radiating impurity.

1. Introduction

Divertor modelling with the B2-Eirene code package [1, 2] has become an essential tool in the ITER design. This code, constantly validated against data from various experiments, predicts particular features of divertor plasma performance in ITER, and similar features can be found in the experiments on JET and other divertor tokamaks. This gives credibility to the results of modelling which are used in the design. In particular, a V-shaped target and efficient gas transfer between the inner and outer divertors are features of the latest ITER divertor design [3].

A detailed study of the operational window of the ITER divertor for the simplest divertor geometry with carbon targets was presented in [4]. Here we concentrate on the effects of the geometry variation and of the selection of the seeded impurity which are important in optimisation of the divertor design. The broad range of divertor geometries considered precluded a comprehensive study of divertor performance for all of these geometries in the time available. The results of [4] however demonstrate that an acceptable operational window for the starting configuration exists, thus providing the basis for the optimisation studies presented here. In the present work, the plasma consists of DT, He, and either intrinsic C or seeded Ne, Ar, or N ions, with one fluid per charge state and modelling conditions similar to those in [5, 6].

2. Effect of Divertor Target Geometry

It was found in [4] that the peak power loads on the divertor targets depend strongly on the arrangement of the divertor target, dump target, and the bottom part of the divertor chamber. If the bottom part of the divertor chamber makes a distinct corner (“V” shape) with the target, and if the separatrix strike-point is located near this corner, then the neutrals become locked in the vicinity of the strike-point thus favouring partial detachment at the separatrix. The results are consistent with experiments at JET for which the strike point was swept across the target

[7, 8]. The effect is strong: introduction of a “V” about 10 cm deep near the separatrix strike-point, Fig. 1, reduces the peak power load by 30% compared with a straight vertical target for ITER-FEAT, see Fig. 2. This can outweigh the effect of the variation of the divertor length or the divertor closure. Optimisation of the divertor geometry and pumping speed reduces the power loading further (“new V” in Fig. 2). A reduction of the pumping speed causes a similar effect, i.e. increased neutral pressure in the divertor and reduced power load, but leads to a deterioration of helium removal – which is not the case for our modification of the target shape. Note that the results for the “new V” in Fig. 2 are obtained with realistic gas conductance through the dome structures (see the next Section).

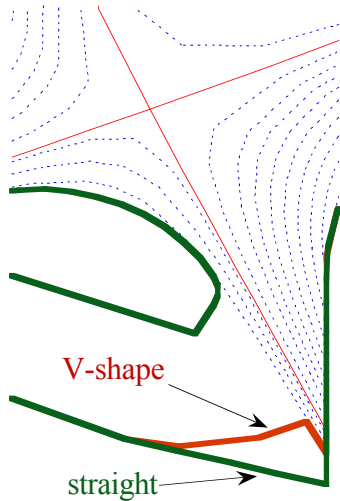


FIG. 1. Variation of the divertor geometry used to study the effect of the “V”.

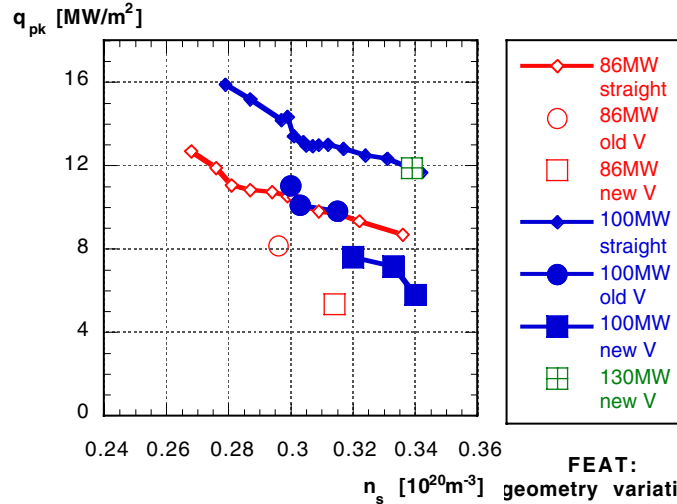


FIG. 2. Variation of the peak power loading of the target for three values of the power entering the SOL. The two V-shaped configurations here are shown in Fig. 1 (“old V”) and Fig. 3 (“new V”).

3. Effect of Gas Conductance between the Divertors

Gas conductance in the private flux region (PFR) between the inner and outer divertors also plays an important role. Indeed, because the neutral pressure in the inner divertor is normally higher than in the outer, the resultant gas flow between the divertors increases the neutral-induced energy loss in the outer divertor and thus reduces the power loading there. In a real divertor, there are supporting structures beneath the dome which hinder the gas flow. This effect was modelled by introducing two semi-transparent surfaces connecting the dome edges with the divertor bottom, Fig. 3. The transparency of these surfaces – that is, the probability ζ that a particle impinging on the surface traverses it – was varied between 1 (equivalent to the previous geometry) and 0 (divertors closed to the PFR). The results are shown in Fig. 4 where the peak power loading is plotted against the upstream density for different values of ζ . The effect is clearly seen: reduction of the gas conductance between the divertors results on the whole in a considerable increase of the peak power loading (with saturation seen at $\zeta = 0.25$ to 0.1). Comparison with a two-chamber model shows that the dome conductance prevails over the transparent wall conductance at $\zeta > 0.5$.

The decrease of peak power loading in the modelling is consistent with the JET experiments [9], where the introduction of a “septum” separating the inner and outer divertors was found to increase the asymmetry of the divertor parameters, i. e., the outer divertor became hotter and the inner one more detached. In that experiment, it was found that symmetry of the divertor parameters can be recovered by gas puffing in the outer divertor and pumping from

the inner. This approach does not however look feasible in ITER: the gas throughput between the divertors at $\zeta = 1$ is calculated to be 300 to 400 Pa·m³/s, far beyond the pumping capability of ITER (the DT throughput of 100 to 200 Pa·m³/s). Sufficient gas conductance between the divertors in the PFR should therefore be provided in ITER, and the latest divertor design [3] corresponds to $\zeta = 0.56$ (the value used for the “new V” results in Fig. 2).

For the pumping speed available in ITER, the modelling reveals a net influx to the PFR from the inner divertor and a net outflow from the PFR toward the pump and toward the outer divertor, both for DT and helium (see the neutral flow pattern indicated in Fig. 3). This means that there is no net pumping from the outer divertor. Hence, one could, in principle, optimise the divertors following different criteria, power handling for the outer and pumping for the inner, although this optimisation is not straightforward. The conditions for helium pumping in the inner divertor also depend on the plasma temperature there, drastically degrading when the temperature goes up. The helium concentration upstream shows no strong variation with ζ and slightly decreases in some cases along with ζ . This is again consistent with pumping from the inner divertor. Indeed, a reduction of gas throughput increases the pressure in the inner divertor and improves somewhat the conditions for helium pumping.

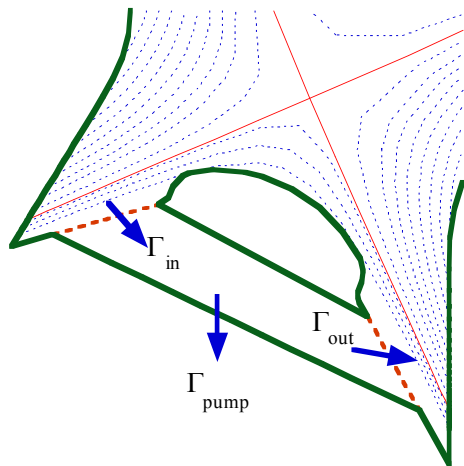


FIG. 3. Model geometry used for the gas conductance study. Thick dashed lines show the semi-transparent liner surfaces and arrows a typical neutral flow pattern.

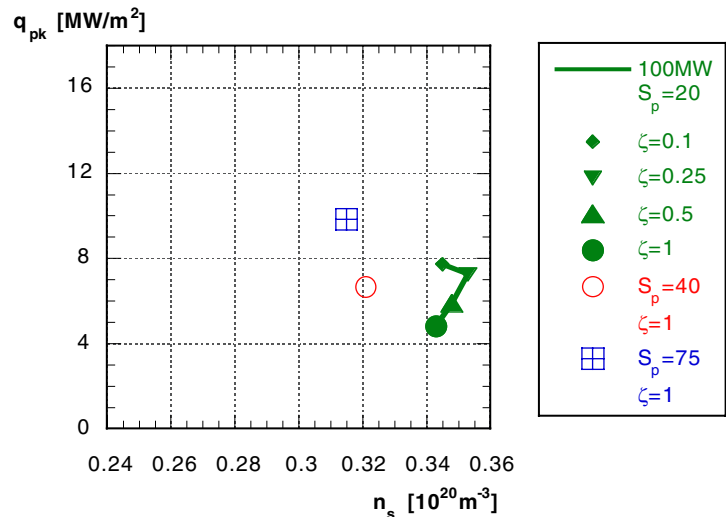


FIG. 4. Peak power vs. upstream density for V-shaped target. Input power 100 MW, varying pumping speed S_p (m³/s). ζ is the probability that a neutral particle impinging on the liner under the dome traverses it.

4. Effect of Impurity Seeding

At present, one cannot exclude the possibility that the magnitude of tritium co-deposition [3] might lead to the exclusion of carbon as a plasma-facing material. In that case, an alternative scenario will have to be found in which a sufficient radiation level in the edge plasma is provided by seeding additional impurities. The trade-off here is between sufficiently high radiation power and sufficiently low Z_{eff} in the plasma core. The first modelling results for the ITER-FEAT divertor have shown that replacement of carbon with neon has a minor negative effect on the operational window, increasing Z_{eff} [4]. To provide an initial evaluation of optimisation potential of the impurity seeding scheme, several modelling runs without carbon and with different seeded impurities (Ne, Ar, N) have been done. In this model, the gaseous

impurities were injected in the outer divertor from the PFR side and zero particle flux across the innermost closed flux surface (CEI: core-edge interface) was specified as the boundary condition for each impurity charge state. This makes the model more numerically stable and physically consistent. Indeed, now there are no impurity sinks or sources in the core. In [4, 6], this was also the case for carbon but not for neon, for which the Ne^{10+} density at the CEI was fixed corresponding to a somewhat unphysical neon source in the core. The results are shown in Fig. 5 where the peak power load and radiated power vs. upstream plasma density and Z_{eff} at the CEI vs. DT throughput are compared with those for the non-seeded divertor operation. The general trend is that the higher the Z_{eff} , the lower the peak power – almost independent of the radiating impurity selection (compare argon with neon and carbon with nitrogen in Fig. 5). The increase of Z_{eff} observed when neon is fed from the core, Fig. 5, can be attributed to the build-up of a gradient of the neon density inside the separatrix, which would be necessary to maintain the neon influx. The overall result is consistent with [10] (radiation from impurity-seeded discharges depends only weakly on the kind of seeded impurity). The carbon cases have higher radiated power but still have higher peak power load. The radiation is emitted much closer to the divertor plate, contributing 4 MW/m^2 to the peak power load on the outer divertor for the carbon cases compared to <0.4 for the impurity-seeded cases.

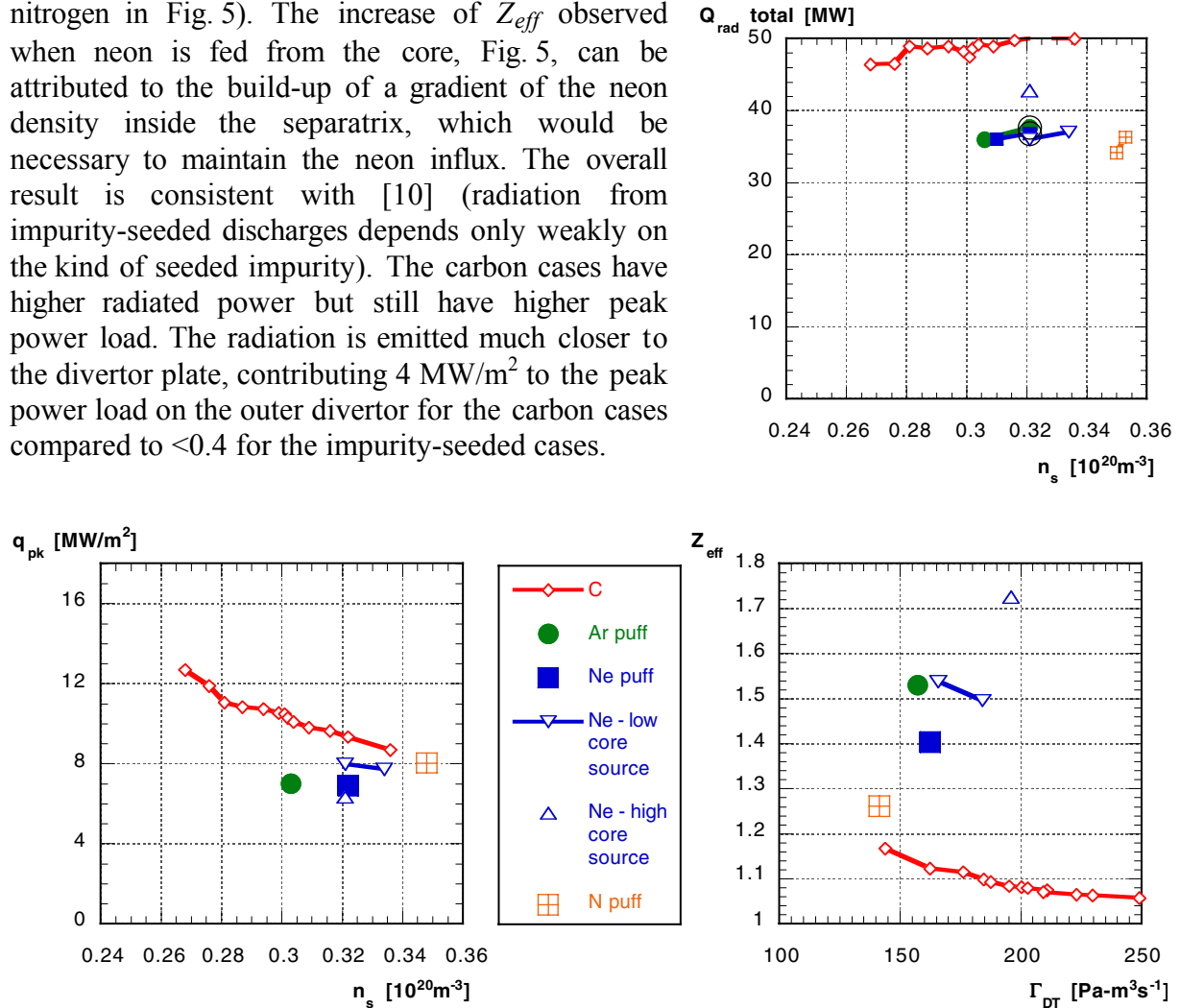


FIG. 5. Divertor performance with impurity seeding: peak power loading (left) and radiated power (top right) vs. upstream plasma density and Z_{eff} at the core-edge interface vs. DT particle throughput (right). The curve corresponding to the intrinsic carbon impurity as the radiator is also shown for comparison. The input power is 86 MW, pumping speed $75 \text{ m}^3/\text{s}$, straight target.

5. Conclusions and Discussion

An acceptable operational window for the ITER-FEAT divertor in inductive operation has been recently identified [4]. Further studies aimed at divertor optimisation are in progress and initial results relevant to the ITER design are reported in the present paper.

A V-shaped configuration of the target and divertor floor is beneficial for divertor performance, providing a considerable reduction of the peak power load on the target without adversely affecting the helium removal. The effect is mostly due to accumulation of neutrals near the strike point when the "V" is plugged by plasma, as confirmed by the available experimental data from JET. Such a configuration could also be useful for transients such as ELMs, attenuating the increased power load at the targets. However, it can negatively affect the operational flexibility of the machine by reducing the freedom of positioning the strike point. On balance, as a result of these studies, a V-shaped target is foreseen for ITER.

Efficient particle exchange between the inner and outer divertors via neutral gas in the PFR is essential to achieve an acceptable operational regime for the ITER divertor. The transparency of the walls should be above 0.5. The high gas throughput between the divertors, typically above 300 Pa·m³/s, enhances the neutral-induced power dissipation in the outer divertor thus reducing the peak power load there. These results are consistent with the JET experiment using the "septum" in the divertor, and the latest divertor design [3] takes them into account.

Impurity seeding can be used as an alternative to natural carbon radiation if the use of carbon were to become undesirable because of tritium co-deposition. Different radiating impurities can be used. In impurity seeding, the main trade-off is between the radiated power and Z_{eff} at the CEI, and the first results suggest that this trade-off is not strongly affected by the choice of impurity. The impurity-seeded cases investigated have lower total radiation but nevertheless lower peak power load than the carbon cases because the radiation is emitted further from the divertor plate. The radiation contribution to the peak power load is considerable for the former, and small for the latter. Further work on impurity seeding is required, among other considerations, to determine the maximum density (e.g. X-point Marfe).

Further work is in progress to study the compatibility of acceptable divertor performance with steady-state operation using non-inductive current drive in ITER, which requires a higher power entering the scrape-off layer at a lower upstream plasma density.

References

- [1] D. Reiter, H. Kever, G.H. Wolf, et al., Plasma Phys. and Contr. Fusion, **33** (1991) 1579.
- [2] R. Schneider, D. Reiter, H.-P. Zehrfeld, et al. J. Nucl. Mater., **196–198** (1992) 810.
- [3] G. Janeschitz, et al., "Divertor Design and Its Integration into the ITER Machine", this conference.
- [4] A. S. Kukushkin, G. Janeschitz, A. Loarte, et al., "Critical Issues in Divertor Optimisation for ITER-FEAT", Proc. 14th PSI Conference, Rosenheim, 2000 (to be published in J. Nucl. Mater.)
- [5] H. D. Pacher, A. S. Kukushkin, D. P. Coster, et al. J. Nucl. Mater., **266–269** (1999) 1172.
- [6] A. S. Kukushkin, H. D. Pacher, D. P. Coster, et al., Fusion Energy 1998 (Proc. 17th Conference, Yokohama, 1998), IAEA, Vienna, 1999, p. 1013
- [7] A. Loarte, Nucl. Fusion **38** (1998) 587.
- [8] R. Monk, et al., Proc. 24th EPS Conf. Contr. Fusion Plasma Phys., Berchtesgaden, 1997, Vol. 21A, p. 117.
- [9] C. F. Maggi, et al., "Effect of D₂ Fuelling Location in JET MkII Gas Box Divertor Discharges", Proc. 26th EPS Conf. on Contr. Fusion and Plasma Phys., Maastricht, 1999, ECA Vol. 23J (1999) 201.
- [10] G. F. Matthews, et al., Nuclear Fusion, **39** (1999) 19.